Incorporation of luminescent CdSe/ZnS core-shell quantum dots and PbS quantum dots into solution-derived chalcogenide glass films

Spencer Novak,[1,2,*] Luca Scarpantonio,[2] Jacklyn Novak,[1,2] Marta Dai Prè,[3] Alessandro Martucci,[3] Jonathan D. Musgraves,[1] Nathan D. McClenaghan,[2] and Kathleen Richardson[1,4]

[1]*School of Materials Science and Engineering, COMSET, Clemson University, Clemson, SC 29634, USA*
[2]*Univ. Bordeaux, ISM, CNRS UMR 5255, F-33400 Talence, France*
[3]*INSTM and Dipartimento di Ingegneria Industriale, Università di Padova, Padova, Italy*
[4]*College of Optics and Photonics, CREOL, University of Central Florida, USA*
**spencen@g.clemson.edu*

Abstract: CdSe/ZnS core-shell quantum dots (CSQDs) and PbS quantum dots (QDs) were synthesized using a colloidal method and incorporated into $Ge_{23}Sb_7S_{70}$ glass films via a solution-derived approach to film formation. Photoluminescence (PL) from the QDs inside the glass matrix was observed in the visible (CdSe/ZnS) and near-IR (PbS) regions. Properties of the QDs were found to be environment dependent, with the amine solvent partially quenching the luminescence. The PL lifetime of the CdSe/ZnS CSQDs and PbS QDs in the glass film was decreased to varying degrees from that of the QDs in pure chloroform. Monitoring the steady-state PL intensity and luminescence lifetime of PbS doped films showed that appropriate heat treatment of the deposited film increases the luminescence efficiency by removing residual solvent from the glass matrix.

OCIS codes: (160.2750) Glass and other amorphous materials; (310.6860) Thin films, optical properties; (160.4236) Nanomaterials; (160.2540) Fluorescent and luminescent materials.

References and links

1. D. Bera, L. Qian, T.-K. Tseng, and P. H. Holloway, "Quantum dots and their multi-modal applications: a review," Materials **3**(4), 2260–2345 (2010).
2. L. Bakueva, S. Musikhin, M. A. Hines, T.-W. F. Chang, M. Tzolov, G. D. Scholes, and E. H. Sargent, "Size-tunable infrared (1000–1600 nm) electroluminescence from PbS quantum dot nanocrystals in a semiconducting polymer," Appl. Phys. Lett. **82**(17), 2895–2898 (2003).
3. J. M. Pietryga, R. D. Schaller, D. Werder, M. H. Stewart, V. I. Klimov, and J. A. Hollingsworth, "Pushing the band gap envelope: mid-infrared emitting colloidal PbSe quantum dots," J. Am. Chem. Soc. **126**(38), 11752–11753 (2004).
4. W. Heiss, E. Kaufmann, M. Böberl, T. Schwarzl, G. Springholz, G. Hesser, F. Schäffler, K. Koike, H. Harada, M. Yano, R. Leitsmann, L. E. Ramos, and F. Bechstedt, "Highly luminescent nanocrystal quantum dots fabricated by lattice-type mismatched epitaxy," Physica E **35**(2), 241–245 (2006).
5. V. Hamel, J. Fick, É. J. Knystautas, R. Vallée, A. Villeneuve, F. Schiettekatte, S. Roorda, C. Lopez, and K. A. Richardson, "Photoluminescence in rare-earth-doped chalcogenide thin films," Optical Amplifiers and Their Applications, A. Mecozzi, M. Shimizu, and J. Zyskind, eds., Vol. 44 of OSA Trends in Optics and Photonics (Optical Society of America, 2000), paper OMD6.
6. E. N. Borisov, V. B. Smirnov, A. Tverjanovich, and Yu. S. Tveryanovich, "Deposition of Er^{3+} doped chalcogenide glass films by excimer laser ablation," J. Non-Cryst. Solids **326–327**, 316–319 (2003).
7. V. Lyubin, M. Klebanov, B. Sfez, and B. Ashkinadze, "Photoluminescence and photodarkening effect in erbium-doped chalcogenide glassy films," Mater. Lett. **58**(11), 1706–1708 (2004).
8. P. K. Dwivedi, Y. W. Sun, Y. Y. Tsui, D. Tonchev, M. Munzar, K. Koughia, C. J. Haugen, R. G. DeCorby, J. N. McMullin, and S. O. Kasap, "Rare-earth doped chalcogenide thin films fabricated by pulsed laser deposition," Appl. Surf. Sci. **248**(1-4), 376–380 (2005).
9. V. Lyubin, M. Klebanov, B. Sfez, M. Veinger, R. Dror, and I. Lyubina, "Photoluminescence, photostructural transformations and photoinduced anisotropy in rare-earth-doped chalcogenide glassy films," J. Non-Cryst. Solids **352**(9-20), 1599–1601 (2006).

#185362 - $15.00 USD Received 19 Feb 2013; revised 29 Apr 2013; accepted 30 Apr 2013; published 6 May 2013

10. K. Yan, R. Wang, K. Vu, S. Madden, K. Belay, R. Elliman, and B. Luther-Davies, "Photoluminescence in Er-doped Ge-As-Se chalcogenide thin films," Opt. Mater. Express **2**(9), 1270–1277 (2012).
11. B. J. Eggleton, B. Luther-Davies, and K. Richardson, "Chalcogenide photonics," Nat. Photonics **5**, 141–148 (2011).
12. J. Hu, V. Tarasov, N. Carlie, N. N. Feng, L. Petit, A. Agarwal, K. Richardson, and L. Kimerling, "Si-CMOS-compatible lift-off fabrication of low-loss planar chalcogenide waveguides," Opt. Express **15**(19), 11798–11807 (2007).
13. N. Carlie, J. D. Musgraves, B. Zdyrko, I. Luzinov, J. Hu, V. Singh, A. Agarwal, L. C. Kimerling, A. Canciamilla, F. Morichetti, A. Melloni, and K. Richardson, "Integrated chalcogenide waveguide resonators for mid-IR sensing: leveraging material properties to meet fabrication challenges," Opt. Express **18**(25), 26728–26743 (2010).
14. J. D. Musgraves, N. Carlie, J. Hu, L. Petit, A. Agarwal, L. C. Kimerling, and K. A. Richardson, "Comparison of the optical, thermal and structural properties of Ge-Sb-S thin films deposited using thermal evaporation and pulsed laser deposition techniques," Acta Mater. **59**(12), 5032–5039 (2011).
15. S. Song, N. Carlie, J. Boudies, L. Petit, K. Richardson, and C. B. Arnold, "Spin-coating of $Ge_{23}Sb_7S_{70}$ chalcogenide glass thin films," J. Non-Cryst. Solids **355**(45-47), 2272–2278 (2009).
16. M. Waldmann, J. D. Musgraves, K. Richardson, and C. B. Arnold, "Structural properties of solution processed $Ge_{23}Sb_7S_{70}$ glass materials," J. Mater. Chem. **22**(34), 17848–17852 (2012).
17. J. Novak, S. Novak, M. Dussauze, E. Fargin, F. Adamietz, J. D. Musgraves, and K. Richardson, "Evolution of the structure and properties of solution-based $Ge_{23}Sb_7S_{70}$ thin films during heat treatment," Mater. Res. Bull. **48**(3), 1250–1255 (2013).
18. J. Hu, V. Tarasov, N. Carlie, R. Sun, L. Petit, A. Agarwal, K. Richardson, and L. Kimerling, "Low-loss integrated planar chalcogenide waveguides for microfluidic chemical sensing," Proc. SPIE **6444**, 64440N (2007).
19. J. Hu, M. Torregiani, F. Morichetti, N. Carlie, A. Agarwal, K. Richardson, L. C. Kimerling, and A. Melloni, "Resonant cavity-enhanced photosensitivity in As_2S_3 chalcogenide glass at 1550 nm telecommunication wavelength," Opt. Lett. **35**(6), 874–876 (2010).
20. C. Tsay, E. Mujagić, C. K. Madsen, C. F. Gmachl, and C. B. Arnold, "Mid-infrared characterization of solution-processed As_2S_3 chalcogenide glass waveguides," Opt. Express **18**(15), 15523–15530 (2010).
21. J. Wüsten and K. Potje-Kamloth, "Chalcogenides for thin film NO sensors," Sens. Actuators B Chem. **145**(1), 216–224 (2010).
22. T. Petkova, C. Popov, T. Hineva, P. Petkov, G. Socol, E. Axente, C. N. Mihailescu, I. N. Mihailescu, and J. P. Reithmaier, "Characterization of pulsed laser deposited chalcogenide thin layers," Appl. Surf. Sci. **255**(10), 5318–5321 (2009).
23. J. Hu, N. Carlie, L. Petit, A. Agarwal, K. Richardson, and L. Kimerling, "Demonstration of chalcogenide glass racetrack microresonators," Opt. Lett. **33**(8), 761–763 (2008).
24. A. Ganjoo, H. Jain, C. Yu, R. Song, J. V. Ryan, J. Irudayaraj, Y. J. Ding, and C. G. Pantano, "Planar chalcogenide glass waveguides for IR evanescent wave sensors," J. Non-Cryst. Solids **352**(6-7), 584–588 (2006).
25. I. D. Tolmachov, A. V. Stronski, and M. Vlcek, "Optical properties and structure of As-Ge-Se thin films," Semicond. Phys. Quantum Electron. Optoelectron. **13**, 276–279 (2010).
26. V. Balan, C. Vigreux, A. Pradel, A. Llobera, C. Dominguez, M. I. Alonso, and M. Garriga, "Chalcogenide glass-based rib ARROW waveguide," J. Non-Cryst. Solids **326–327**, 455–459 (2003).
27. M. V. Kovalenko, R. D. Schaller, D. Jarzab, M. A. Loi, and D. V. Talapin, "Inorganically functionalized PbS-CdS colloidal nanocrystals: integration into amorphous chalcogenide glass and luminescent properties," J. Am. Chem. Soc. **134**(5), 2457–2460 (2012).
28. M. Amelia, A. Lavie-Cambot, N. D. McClenaghan, and A. Credi, "A ratiometric luminescent oxygen sensor based on a chemically functionalized quantum dot," Chem. Commun. (Camb.) **47**(1), 325–327 (2010).
29. I. Moreels, K. Lambert, D. Smeets, D. De Muynck, T. Nollet, J. C. Martins, F. Vanhaecke, A. Vantomme, C. Delerue, G. Allan, and Z. Hens, "Size-dependent optical properties of colloidal PbS quantum dots," ACS Nano **3**(10), 3023–3030 (2009).
30. L. Petit, N. Carlie, F. Adamietz, M. Couzi, V. Rodriguez, and K. C. Richardson, "Correlation between physical, optical and structural properties of sulfide glasses in the system Ge-Sb-S," Mater. Chem. Phys. **97**(1), 64–70 (2006).
31. P. Thanasekaran, R.-T. Liao, B. Manimaran, Y.-H. Liu, P.-T. Chou, S. Rajagopal, and K. L. Lu, "Photoluminescence electron-transfer quenching of rhenium(I) rectangles with amines," J. Phys. Chem. A **110**(37), 10683–10689 (2006).
32. K. Kang and K. Daneshvar, "Matrix and thermal effects on photoluminescence from PbS quantum dots," J. Appl. Phys. **95**(9), 4747–4751 (2004).
33. B. Ma, C. E. Bunker, R. Guduru, X.-F. Zhang, and Y.-P. Sun, "Quantitative spectroscopic studies of the photoexcited state properties of methano- and pyrrolidino-[60]fullerene derivatives," J. Phys. Chem. A **101**(31), 5626–5632 (1997).
34. A. P. Losev, I. M. Byteva, and G. P. Gurinovich, "Singlet oxygen luminescence quantum yields in organic solvents and water," Chem. Phys. Lett. **143**(2), 127–129 (1988).

#185362 - $15.00 USD Received 19 Feb 2013; revised 29 Apr 2013; accepted 30 Apr 2013; published 6 May 2013

1. Introduction

QDs are semiconductor nanoparticles with many attractive properties, such as high photostability and broad, tunable emission that can extend from the visible to the mid-IR, depending on the size and composition of the QD [1–4]. Due to quantum confinement effects, smaller QDs emit shorter wavelengths of light than larger QDs of the same composition. This characteristic allows the position of the luminescence band to be adjusted simply by tuning the size of the QD, an advantage over emission from rare-earth ions, which have been studied in chalcogenide glass films for luminescent properties in references [5–10].

This study investigates the incorporation of two well-studied QDs into solution-derived chalcogenide glass (ChG) films, visibly emitting core-shell CdSe/ZnS and near-IR emitting PbS. ChGs are widely known for their transparency to IR light, low phonon energies and low glass transition temperature (T_g), making them suitable for drawing fibers and molding lenses for use in mid-IR optical systems [11]. Additionally, films of ChGs are attractive for the fabrication of chemical sensing devices operating in the infrared, where many organic compounds have an optical signature [12,13]. Such a sensing device typically contains three main components, a source of light, a ChG film resonator where the analyte interacts with the light, and a detector which senses changes in absorption and/or shifts in the resonant wavelength due to a binding event. ChG bus waveguides connect these components and provide the route for light transmission between each component. ChG film fabrication and waveguide deposition is currently an area of high interest [12–26]. However, current sensors have only been demonstrated using quantum cascade lasers or other external to the chip components as the light source. The present work investigates QD incorporation into ChG films as a low-cost, easy to manufacture source of light for a sensing device. Several different methods to deposit films of ChG have been demonstrated, such as sputtering, pulsed laser deposition, and thermal evaporation [12,14,26]. However, a solution-derived approach [15–17] offers the potential to easily incorporate dispersed nanoparticles, such as QDs, into the film by mixing a solution of nanoparticles with a solution of glass before spin-coating the film. Currently, to the best of our knowledge, there is only one publication to date which investigates QD incorporation in solution-derived chalcogenide glass films [27]. In this study by Kovalenko et al, PbS/CdS CSQDs were inorganically functionalized with AsS_3^{3-} ions, allowing high levels of QDs to be dispersed in an As_2S_3/propylamine solution, with strong PL from the deposited films. In our study, we report PL from simple, organically capped QDs in $Ge_{23}Sb_7S_{70}$ films, which could be successfully prepared, despite minor issues with long-term solubility (>30 min) of the QDs in the glass solution, and also investigate the effect of film heat treatment on PL intensity.

Solution-derived $Ge_{23}Sb_7S_{70}$ glass films were doped with CdSe/ZnS CSQDs and PbS QDs to demonstrate luminescence over a large range of wavelengths and to further investigate the principles of how nanoparticles interact in solution-based ChG film processing. QD solutions were titrated with propylamine, the glass solvent, to determine its effect on QD luminescence properties. CdSe/ZnS CSQD-doped glass films were deposited and characterized using luminescence lifetime measurements and steady-state photoluminescence (PL) spectra. PbS QD-doped films were deposited using varying concentrations of QDs, and the effect of different heat treatments on the integrated intensity of steady-state PL spectrum and luminescence lifetime was studied.

2. Experimental procedure

2.1 Synthesis of QDs

CdSe/ZnS CSQDs capped with tri-n-octyl-phosphine oxide (TOPO) were synthesized with core diameter of 5.8 nm and total diameter of 7.9 nm using the method described by Amelia et al [28]. PbS QDs were synthesized via a reaction of lead (II) acetate trihydrate with thioacetamide in anhydrous methanol in an argon purged Schlenk line. 0.4 g (1.23 mmol) lead

#185362 - $15.00 USD Received 19 Feb 2013; revised 29 Apr 2013; accepted 30 Apr 2013; published 6 May 2013

acetate was dissolved in 5 mL anhydrous methanol with stirring. 0.8 mL acetic acid was added, and then 0.06 g (0.292 mmol) thioctic acid dissolved in 1 mL methanol was added dropwise. In a separate flask, 0.09 g (1.19 mmol) thioacetamide was dissolved in 2 mL anhydrous methanol, and added rapidly to the lead acetate solution to nucleate PbS particles in a short range of time. The solution turned from clear to dark brown over a period of about 10 min, and was left to react at room temperature under vigorous stirring for 2 hrs 15 min. The QDs were then precipitated from the methanol with 15 mL acetone per mL of reaction solution and centrifuged at 3000 rpm for 10 min. The precipitate was washed by replacing the acetone twice, scraping the QDs off the side of the flask if necessary. They were then redispersed in chloroform and washed twice to remove the acetone. About 15 μL of 1-dodecanethiol per mL of reaction solution was used as a stabilizer. The concentration of the PbS QD solutions was estimated by drying a known volume of solution under vacuum for 3-4 hrs and weighing the precipitate. Based on the position of the luminescence band of the PbS QDs, the diameter was estimated to be 3.3 nm [29].

2.2 Fabrication of $Ge_{23}Sb_7S_{70}$ glass and QD-doped films

Bulk $Ge_{23}Sb_7S_{70}$ glass was prepared by batching elemental five nine (5N) pure materials into a fused silica ampoule inside of a nitrogen-purged glove box using techniques discussed in detail in [30] to prepare bulk glass materials for subsequent solution-based film formation. The ampoule was vacuum sealed (10^{-5} torr) for 4 hours at 90 °C to drive off any residual moisture, then sealed using a gas-oxygen torch. The batch was melted for 15 hours at 925 °C in a rocking furnace to ensure homogeniety, air-quenched, and annealed at 271 °C, 40 °C below the T_g of the glass [30].

$Ge_{23}Sb_7S_{70}$ films doped with QDs were fabricated using the following steps:

1. Dissolution of glass crushed by mortar and pestle in propylamine solvent with concentration of 0.05 g/mL.
2. Mixing QD solution with glass solution in 1:2 ratio by volume. Solutions were doped with 0.35 μM CdSe/ZnS CSQDs. Varying concentrations of PbS QD solution (1.7, 8.6 and 17 μM) was used to vary the concentration of QDs in the deposited film.
3. Within 10 s after mixing the QD and glass solutions, films were deposited by spin-coating on a borosilicate or silicon substrate at 3000 rpm for 10 s.
4. Heat treatment of the film in dry air to drive residual solvent from the film matrix.

Film heat treatments are detailed in Table 1. These sequential heat treatments were chosen based on our study of undoped solution-derived films of the same glass composition, and optimized such that residual solvent, as determined by the size of the propylamine absorption band at 2960 cm^{-1}, was minimized [17].

Table 1. Heat Treatments Used for PbS Doped $Ge_{23}Sb_7S_{70}$ Films

Heat Treatment	Description
HT0	5 min @ 100°C
HT1	30 min @ 100°C
HT2	30 min @ 100°C
HT3	20 min @ 160°C
HT4	20 min @ 180°C
HT5	20 min @ 200°C

2.3 Characterization of QD-doped films

Film RMS roughness was determined with a Zygo NewView white light interferometer. Transmission spectra were taken in the mid-IR using a Nicolet 6700 FT-IR with a resolution of 8 cm^{-1} and 100 acquisitions. Steady-state PL spectra, fluorescence lifetimes, and quantum

#185362 - $15.00 USD Received 19 Feb 2013; revised 29 Apr 2013; accepted 30 Apr 2013; published 6 May 2013

yields were obtained using a Horiba Jobin-Yvon Fluorolog-3 spectrofluorimeter. In these experiments, the excitation source was either a 450 W Xenon lamp with a double monochromator or a Nd:YAG laser (λ = 532 nm): a Nanolase (12 kHz) or Innolas Picolo-AOT 1-MOPA. Detection of infrared luminescence was achieved using a Hamamatsu 10330-45 photomultiplier, while detection of visible luminescence was with a Hamamatsu R2658P PMT. Lifetimes were taken at the peak luminescence wavelength via the time-correlated single photon counting method using a 1 MHz, 460 nm pulsed nano-LED excitation source in the visible or using a Fastcom P7889 multiscaler acquisition card operating with a 10 GHz sweep rate in the NIR. Absolute quantum yield values of CdSe/ZnS CSQDs in the visible were determined by taking spectra using a Labsphere optical Spectralon integrating sphere with diameter of 100 mm, providing a reflectance of >99% over the 400-1500 nm range, and >95% within 250-2500 nm range. The quantum yield of PbS QDs in the near-IR was estimated by comparing the integrated area of the steady-state emission spectrum to that of singlet oxygen generated by a C_{60} photosensitizer dissolved in toluene. Both solutions were diluted such that they had the same absorbance at the excitation wavelength of 532 nm.

3. Results and discussion

3.1 Effect of propylamine on QD properties

The effect of propylamine (glass solvent) on the QDs was first investigated by titrating the QD solution with propylamine. Strong luminescence quenching was observed as a function of the increasing amine concentration, with a Stern-Volmer analysis shown in Fig. 1.

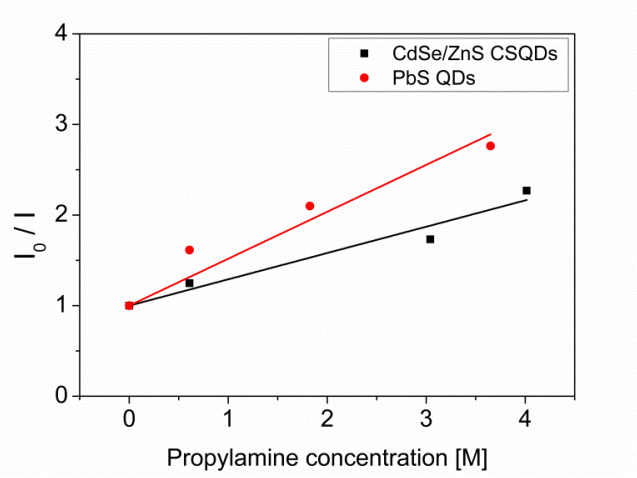

Fig. 1. Stern-Volmer plots of CdSe/ZnS CSQDs and PbS QDs with varying concentrations of propylamine. CdSe/ZnS CSQDs were excited at 500 nm, and PbS QDs were excited at 532 nm. Intensities were taken by integrating steady-state PL spectra, with error approximately 5%.

Amines are well-known to quench luminescence through electron transfer due to the lone-pair of electrons on the nitrogen atom, which is easily oxidized [31]. Shown in Eq. (1), the Stern-Volmer relationship for collisional quenching is given, where I_0 and I are the PL intensities of QDs (dispersed in pure chloroform) with propylamine concentration of 0 and [Q], respectively, and k_{sv} is the Stern-Volmer constant equal to the product of k_q, the quenching rate constant, and τ_0, the unquenched lifetime.

$$\frac{I_0}{I} = 1 + k_{SV}[Q] = 1 + k_q \tau_0 [Q] \quad (1)$$

The Stern-Volmer constant was estimated by the slope of linear trendlines with intercepts fixed at 1. For CdSe/ZnS CSQDs, k_{sv} was found to be 0.29, and for PbS QDs, k_{sv} was found

#185362 - $15.00 USD Received 19 Feb 2013; revised 29 Apr 2013; accepted 30 Apr 2013; published 6 May 2013

to be 0.52. During this testing, the QDs were found to be stable with no aggregation in all mixtures of propylamine and chloroform for several hours. In contrast, when adding QD solution to glass solution, precipitation was observed within 30 minutes. For this reason, films were deposited as quickly as possible, approximately 10 s after mixing the two solutions in order to reduce the time-dependent aggregation. It is proposed that dissolved glass in the solution cleaves the capping agent from the PbS QDs, leading to the aggregation in glass solution but not pure propylamine.

3.2 Comparison of QD PL spectra in various environments

The PL spectrum of a QD-doped film differs from that of the QDs in solution. Figure 2 shows a comparison between CdSe/ZnS CSQDs and PbS QDs in various environments.

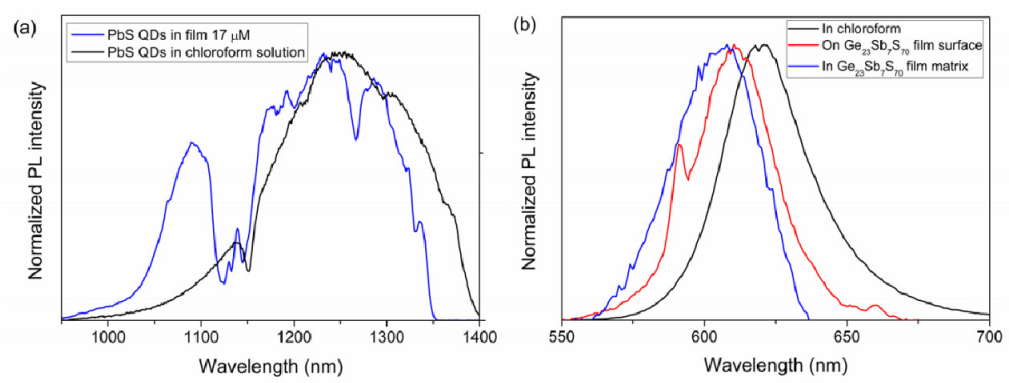

Fig. 2. Comparison of photoluminescence spectrum of (a) PbS QD-doped $Ge_{23}Sb_7S_{70}$ film deposited from a solution containing 17 μM QDs to spectrum of QDs in pure chloroform. The reduction in luminescence intensity at 1150 nm for the QDs in chloroform is due to reabsorption of luminescence, which is also suspected to be responsible for the features at 1125 nm and 1145 nm. Excitation: 532 nm. (b) Comparison of PL spectra of CdSe/ZnS CSQDs dispersed in chloroform to that of CSQDs on film surface and in film matrix. The feature at 590 nm in the spectra of CdSe/ZnS CSQDs on the film surface is a reflection artifact of the instrument. Excitation: 500 nm.

In the case of PbS QDs, there are many features present in the PL spectrum of the doped film. Some of the features, especially those at 1125 nm and 1145 nm, may be attributed to reabsorptions of luminescence caused by residual chloroform in the film matrix. Features could also be caused by the interaction of dissolved glass with the QDs. Glass solution cleaving the capping agent from the QD could result in surface defects responsible for many of the sharp features seen in the luminescence spectrum. These features were not seen when the QD solution was titrated with pure propylamine, so it is likely that they are a result of the impact of glass interaction with the QDs.

Environmental effects on the QD properties are also observed. With both PbS and CdSe/ZnS, the peak luminescence wavelength had blue-shifted from solution to film. For PbS, the peak luminescence wavelength blue-shifts from 1250 nm in chloroform to 1232 nm in the film. For CdSe/ZnS, a progression is seen in the peak luminescence wavelength from 620 nm for QDs in pure chloroform, to 610 nm for QDs deposited on the glass film surface, to 605 nm for QDs in the film matrix. This is believed to be an effect of the presence of the Ge-Sb-S glass on the QD properties, specifically the presence of excess sulfur interaction at the QD surface. This leads to shallow surface states, causing a slight blue-shift in the luminescence band of the QDs, which was studied by Kang et al in reference [32]. The appearance of the peak at 1090 nm in the PL curve of PbS QDs in the film matrix is an artifact of the blue-shift and strong reabsorption features present in the spectrum. It is believed

#185362 - $15.00 USD Received 19 Feb 2013; revised 29 Apr 2013; accepted 30 Apr 2013; published 6 May 2013

that the shape of PL curve of the QDs in the glass matrix would look the same as that of the QDs in chloroform if there were no nearby bonds in the film reabsorbing the luminescence.

3.3 Quantification of PL from QDs in various environments

3.3.1 CdSe/ZnS CSQDs quantum yield and lifetime

The photoluminescence quantum yield was determined for CdSe/ZnS CSQDs on titrating with propylamine to help quantify the effect of the glass solvent on QD properties. Quantum yield (Φ) is defined in Eq. (2).

$$\Phi = \frac{number\ emitted\ photons / \sec}{number\ absorbed\ photons / \sec} \tag{2}$$

It was found that when the CdSe/ZnS CSQDs were in the presence of 33 vol% propylamine, the quantum yield decreased from 0.22 to 0.09. This is consistent with the quenching observed in the steady-state photoluminescence spectra. When these CSQDs were deposited on the more polar glass surface, in the absence of propylamine, the emission quantum yield increased slightly from 0.22 to 0.26, which may be ascribed to less non-radiative de-excitation on blue-shifting, as is generally observed for emission of different chromophores according to Jörtner's energy gap law. Quantum yields of CdSe/ZnS-doped films were unable to be measured due to very low emission. This can be attributed not only to residual solvent quenching but also to a non-negligible spectral overlap between these popular visible-emitting CSQDs and the NIR transmitting, but visible-absorbing ChG, highlighting the more advantageous combination of NIR-emitting PbS quantum dots and ChG. Additionally, it should be noted that in general the inherent waveguiding properties of these films, which leads to a high number of reflections of both excitation and emission light, can affect the calculated quantum yield.

Shown in Fig. 3, lifetimes of CdSe/ZnS CSQDs in various environments were measured in order to investigate the performance of the CSQDs throughout the process of film deposition, and lifetime values given correspond to weighted averages of three decay components, as satisfactory reduced χ^2-values were obtained when fitting CSQD luminescence to triexponential decays.

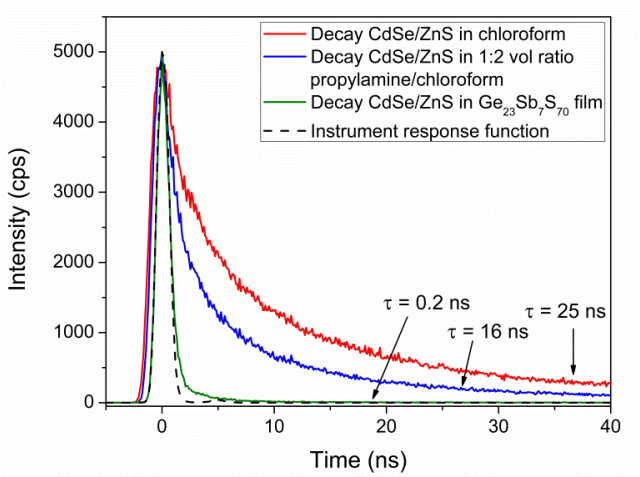

Fig. 3. Photoluminescence decays of CdSe/ZnS CSQDs in various environments and instrument response function, along with deconvoluted luminescence lifetimes, using 460 nm pulsed LED excitation.

It was found that the relative lifetimes of CdSe/ZnS CSQDs in pure chloroform and when titrated with propylamine are consistent with the quantum yield measurements. Indeed,

#185362 - $15.00 USD Received 19 Feb 2013; revised 29 Apr 2013; accepted 30 Apr 2013; published 6 May 2013

assuming an unchanging radiative rate constant in solution the observed luminescence lifetime is anticipated to be proportional to the emission quantum yield. However, the lifetime of the CdSe/ZnS in the film matrix is almost two orders of magnitude less than when titrated with propylamine. This could be explained in two ways: a) significant changes are occurring to the CdSe/ZnS CSQDs due to the film processing, such as aggregation of the CdSe/ZnS CSQDs in the film which would reduce the emission intensity and lifetime; b) electronic energy transfer occurs from the visible-emitting CSQD to the visible-absorbing glass. While the electronic energy transfer theory involving QDs is relatively undeveloped, this non-radiative process would explain the measured simultaneous decrease of luminescence quantum yield and lifetime. The simultaneous lifetime and quantum yield decrease allows us to rule out QD emission followed by glass reabsorption and suggests the radiative rate constant can be of similar magnitude to solution.

3.3.2 Intensity of steady-state PL spectra of PbS and luminescence lifetime changes with varying heat treatments

Because propylamine is known to quench luminescence, the effect of solvent removal by heat treatment of the deposited film on luminescence intensity is very important in order to maximize luminescence efficiency. Ultimately, for envisaged applications, near and mid-IR emitters are more promising, so this experiment was performed exclusively on PbS-doped films of varying dopant concentration. Effects on luminescence lifetime and quantum yield were measured in the near-IR. Relative photoluminescence intensities were determined by integrating the area beneath each steady-state emission spectra, and then plotting vs. heat treatment number, which is shown in Fig. 4.

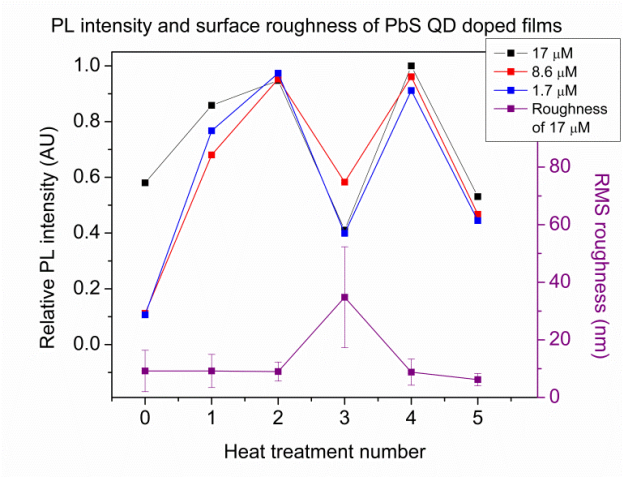

Fig. 4. Plot of photoluminescence intensity of $Ge_{23}Sb_7S_{70}$ films deposited from solutions containing varying concentrations of PbS QDs for various heat treatments.

It was expected that the intensity would continue to increase until no more solvent could be removed from the film, so long as the QDs are not damaged by the heat treatment. Indeed, the initially deposited QD-doped films are a lot less emissive than the quantum dots alone in optically dilute chloroform solution, consistent with a significantly reduced luminescence lifetime (29 ns in the film *cf.* 78 ns in solution). While accurate luminescence quantum yield measurements in the glass films is hampered due to their waveguiding properties, as mentioned above, a net emission decrease is obtained from 0.007 in solution to circa 0.004 in the film, whose value to found to have doubled after HT5. Note: Emission quantum yield values are obtained on comparing with singlet oxygen emission ($\phi_{em} = 1.6 \times 10^{-4}$ in toluene) using a C_{60} photosensitizer [33,34].

#185362 - $15.00 USD Received 19 Feb 2013; revised 29 Apr 2013; accepted 30 Apr 2013; published 6 May 2013

However, the reduced intensity for all films after HT3 is correlated to the RMS roughness of the film surface, and it is believed that the increased roughness scatters the excitation and emission, accounting for the apparent decrease. This hypothesis is reflected in the luminescence lifetime trend, which is largely independent of the number of photons arriving at the detector at low photon fluxes and is found to increase with successive heat treatments. Thus lifetime values measured immediately after HT2 - HT5 are 29 ns, 42 ns, 53 ns and 61 ns, respectively. Considering QD radiative lifetime values, in solution this can be estimated at 9×10^4 s^{-1} (τ = 78 ns), which in the film after HT2 is estimated at 13×10^4 s^{-1} and essentially unchanging at 14×10^4 s^{-1} after HT5. Thus the radiative rate constant in the film is unaffected by heat treatment, while lifetime and quantum yield augment suggesting that a non-radiative process is disfavored on heating which may arise through residual solvent loss. Radiative rate constants of the QDs in the film appear to be of similar magnitude to those in solution, although some limitations are encountered in precise quantum yield determination in these films compared to isotropic solution (*vide supra*).

The PL intensity increases for HT4 due to the reduced surface roughness. For further heat treatments HT5 (which was 20 min at 200 °C) and more, it is suspected that the QDs may have started to be damaged by the high temperature, resulting in lowered emission which may arise from defects that lead to an increased probability of non-radiative de-excitation and lower quantum yields. Equally, following prolonged heat treatment the luminescence lifetime is significantly reduced to a sub-30 ns value, after repeating HT5.

It is also interesting to note that each film reaches approximately the same luminescence intensity at HT2, regardless of PbS QD concentration. This is an indication that there is the same concentration of luminescent QDs in each film, and that there is aggregation occurring, especially for higher concentrations. The TEM images in Fig. 5 confirm the aggregation of the PbS QDs in the films deposited from 17 μM QD concentration.

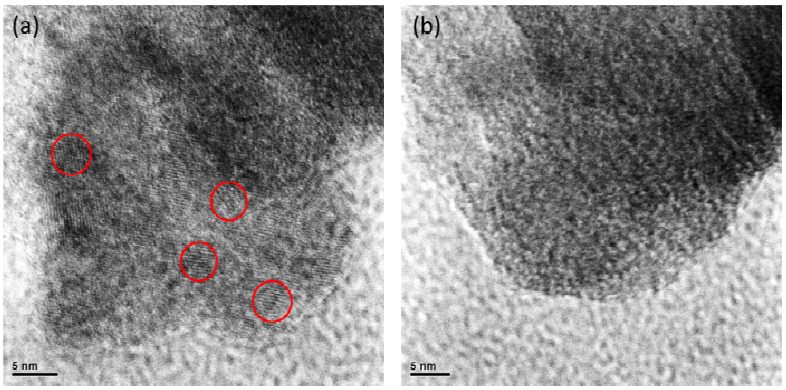

Fig. 5. Transmission electron microscopy of a PbS QD doped $Ge_{23}Sb_7S_{70}$ film. (a) is a region containing an aggregation of QDs, with four individual QDs circled in red as a guide to the eye and (b) is a region of the same film with no QDs.

The QDs were identified by their crystallinity, which is visible in contrast to the amorphous glass film matrix, as well as by their apparent size of about 3 nm. A few of the QDs have been outlined in red to serve as a guide to the eye.

3.4 Infrared transmission spectra

Transmission spectra are shown in Fig. 6 to demonstrate the transparency of the doped films at mid-IR wavelengths, as well as to track the amount of solvent remaining in the films after each heat treatment.

#185362 - $15.00 USD Received 19 Feb 2013; revised 29 Apr 2013; accepted 30 Apr 2013; published 6 May 2013

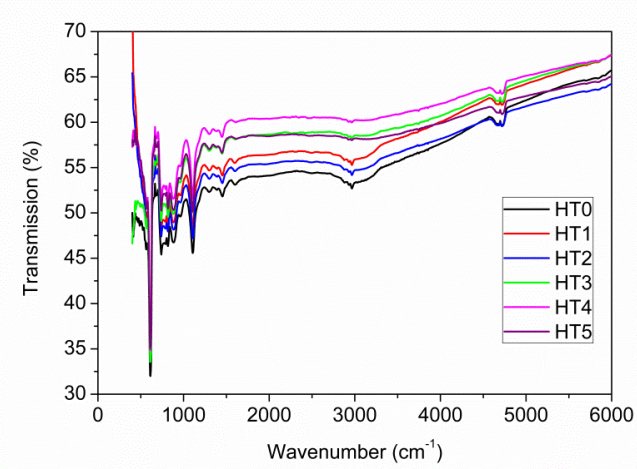

Fig. 6. IR transmission spectra of PbS QD doped $Ge_{23}Sb_7S_{70}$ films deposited from solutions containing 17 μM QD concentration.

The amount of solvent is characterized by the size of the absorption peak centered at 2960 cm^{-1}, which is due to asymmetric stretching of CH_3 groups, and decreases in size for each heat treatment. More details on solvent removal and its effect on the properties of the films can be found in our study of undoped films in reference [17].

4. Conclusions

CdSe/ZnS CSQDs and PbS QDs were incorporated into the matrix of a solution-derived $Ge_{23}Sb_7S_{70}$ film with the observation of photoluminescence in the visible and near-IR, respectively. Both the propylamine solvent and the dissolved glass have effects on the properties of the QDs. Luminescence intensity of NIR-emitting PbS QDs can be improved as much as ten-fold by appropriate heat treating of the film, and there is evidence that the dissolved glass increases the rate of aggregation of the QDs. Similar luminescence properties to solution can be obtained in doped chalcogenide films of these latter species in terms of quantum yield and luminescence lifetime. Dissolved glass also may be responsible for the features in the luminescence spectrum and small blue-shift of the peak emission wavelengths of the QDs from in solution to in the film matrix (15 nm for CdSe/ZnS and 18 nm for PbS).

Acknowledgments

This work is supported by the Defense Threat and Reduction Agency under contract number HDTRA1-10-1-0073 and in part by University of Bordeaux, European Research Council (FP7/2008-2013) grant 208702. This work was also supported by the Atlantis-MILMI program which supports the cooperation between EU and US higher education institutions. Funding support is both provided by the Department of Education of the United States Government under the contract #P116J080033, University of Central Florida and the European Commission under the contract #2008-1750/001-001 CPT-USTRAN, Université Bordeaux 1.